

Gear Tooth Surface Roughness of Helical Gears Manufactured by a Form Milling Cutter

Mattias Svahn, Lars Vedmar, Carin Andersson

Manufacturing involute gears using form grinding or form milling wheels are beneficial to hobs in some special cases, such as small scale production and, the obvious, manufacture of internal gears. To manufacture involute gears correctly the form wheel must be purpose-designed, and in this paper the geometry of the form wheel is determined through inverse calculation. A mathematical model is presented where it is possible to determine the machined gear tooth surface in three dimensions, manufactured by this tool, taking the finite number of cutting edges into account. The model is validated by comparing calculated results with the observed results of a gear manufactured by an indexable insert milling cutter.

Introduction

The dominant and most cost-effective manufacturing method for large scale production of involute gears is hobbing. Nevertheless, form grinding wheels and form milling cutters can be beneficial compared to hobs in some special cases, viz. cheap tooling in rapid prototyping and small scale production, the ability to manufacture internal gears, gear integrated components can be machined complete in one machine and one set-up using multitasking CNC-machine and thereby reducing total lead time and cost. In addition, a new type of form milling cutter has been introduced to the market with indexable carbide inserts which prolong tool life and are capable of operating at higher cutting data, leading to higher productivity.

These tools are not universal, unlike true generating methods such as hobbing and shaping, and therefore must be matched to the gear to cut. When machining spur gears, one can choose from a selection of standard cutters for each module, where each cutter will, at the cost of small geometrical errors to the tooth form, cut a range of gear-tooth numbers. According to Dudley (Ref. 1), these cutters are sometimes used in practice to machine helical gears of small helical angles by matching the cutter to the virtual number of spur gear teeth. However, to machine helical gears correctly, the milling cutter must be purpose designed.

Previous work on machining helical profiles states two problems: 1) the direct problem — to determine the geometry of the manufactured helical profile given the tool geometry, and 2) the inverse problem — to determine the tool geometry that correctly machines the helical profile. One example of solving the direct problem in gear manufacturing is presented by Ishibashi et al. (Ref. 2), who used an element removal method to determine the manufactured gear tooth with given tool geometry. If interference occurred, corrections were made to the tool profile. To solve the inverse problem, the helical profile to machine and the kinematic relation between the workpiece and tool must be specified in advance. This is presented in previous work for helical drill flute machining using a CAD/CAM approach (Refs. 3–4), for helical gear manufacturing by Xiao et al. (Ref. 5) using a contact point method and by Häussler (Ref. 6) using differential geometry. These works derived the tool geometry that correctly machines the helical profile, but did not define the cutting edges to the tool. Thereby no consideration was made of

the machined surface topography. Shih and Chen (Ref. 7) investigated form grinding of helical gears with flank form correction via modifications to the machine tool axis controls and by modification to the tool profile form, using B-splines.

This paper, conversely, focuses on the manufactured tooth surface topography machined by both form milling cutters and form grinding discs where the tool geometry is obtained through inverse calculation. Using a milling cutter, the gear tooth can be finished-cut or rough-cut. If finished-cut, the achieved tooth surface topography is of interest as to how the gear will perform in operation. If the gear is rough-cut instead, additional grinding stock will be left on the involute flank in the milling process to account for feed marks and possible manufacturing errors to be removed in a subsequent refining operation. If the machined surface can be predicted in advance, it opens up for optimization of the manufacturing process, such as minimizing the required amount of grinding stock and choosing process data. The machined tooth surface topography achieved after hobbing is presented by Vedmar (Ref. 8) using parametric differential functions for highest accuracy; this approach will also be used here. The optimal designs of form milling cutters and form grinding wheels are presented and the paper concludes with an experimental verification using a form milling

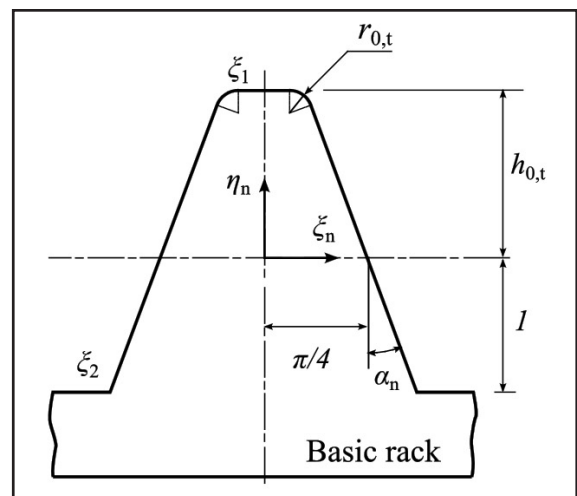


Figure 1 Basic rack.

cutter with carbide inserts.

Geometry of the Tool

One of the intentions in this report is to determine the geometry of a disc-type form tool that should be able to manufacture an involute helical gear correctly. This is achieved through inverse calculation by invoking the geometry of the gear being manufactured and the kinetic relation between work-piece and tool. The geometry of an involute gear can be described through conjugate action with its basic member, in this case the basic rack.

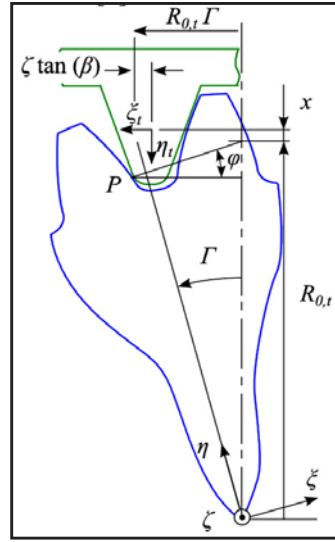


Figure 2 Helical gear conjugated to its basic rack.

Presupposing a gear blank with the outer diameter $2R_{tip}$, and rolling the basic rack with the normal module m_n over the pitch circle $R_t = m_n z / 2 \cos \beta$, the complete gear tooth geometry is determined. The basic rack is described in the normal plane by Vedmar (Ref. 8) using the coordinates ξ_n and η_n (Fig 1). The design of basic racks is standardized for cylindrical gears; see, for example, DIN 867 (Ref. 9).

The basic rack forms the gear tooth in the transverse plane; in this plane the coordinates describing the basic rack are:

$$\xi_t = \frac{\xi_n}{\cos \beta} \quad (1)$$

$$\eta_t = \eta_n$$

In Figure 2 a helical gear is in contact with the basic rack at point P. At any contact, the rack and the gear have a common surface normal, and this normal must be directed through the pitch point. This gives the geometric relation:

$$\Gamma(\xi_n, \zeta) = \frac{-\frac{\xi_n}{\cos \beta} + (\eta_n - x) \cot \varphi + \zeta \tan \beta}{R_{0,t}} \quad (2)$$

and from the rack coordinates we have:

$$\cot \varphi = -\frac{d\eta_t}{d\xi_t} = -\frac{d\eta_n}{d\xi_n} \cos \beta \quad (3)$$

Here, the coordinate ξ_n is chosen as the parameter. By division with the normal module m_n the ideal gear tooth surface is described by the non-dimensional parameters:

$$\mathbf{r} = \begin{pmatrix} \xi(\xi_n, \zeta) \\ \eta(\xi_n, \zeta) \\ \zeta \end{pmatrix} = \begin{pmatrix} R_{0,t} \sin(\Gamma) - \frac{\eta_n - x}{\sin(\varphi)} \cos(\Gamma - \varphi) \\ R_{0,t} \cos(\Gamma) + \frac{\eta_n - x}{\sin(\varphi)} \sin(\Gamma - \varphi) \\ \zeta \end{pmatrix} \quad (4)$$

where $\eta(\xi_n, 0)$ divides the tooth space into two equally symmetric parts. The normal to the gear tooth surface will be needed to determine the point of contact between the tool and the gear tooth surface, and to measure the distance from the ideal smooth tooth surface to the machined surface.

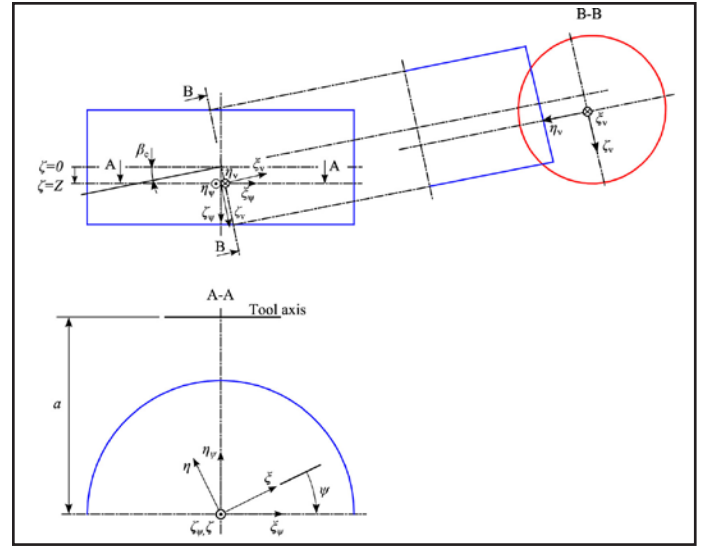


Figure 3 Form wheel and helical gear.

$$\mathbf{n} = \begin{pmatrix} n_\xi \\ n_\eta \\ n_\zeta \end{pmatrix} = \frac{\partial \mathbf{r}}{\partial \xi_n} \times \frac{\partial \mathbf{r}}{\partial \zeta} = \begin{pmatrix} \frac{\partial \eta}{\partial \xi_n} \\ -\frac{\partial \xi}{\partial \xi_n} \\ \frac{\partial \xi}{\partial \xi_n} \frac{\partial \eta}{\partial \zeta} - \frac{\partial \eta}{\partial \xi_n} \frac{\partial \xi}{\partial \zeta} \end{pmatrix} \quad (5)$$

Now the complete geometry of the helical gear tooth is described in detail. To determine the profile of the form wheel tool, which should be able to manufacture this gear correctly, the tool axis is positioned at the center distance a , and at the angle β_c to the transverse plane of the gear (Fig. 3). If a point P_v on the tool is to generate a point P_g on the gear, these must be the same point in space — i.e. $P_v = P_g = P$. In addition, the normal of the gear tooth surface must coincide with the normal to the tool surface in such a point. The point P_g belongs to the gear tooth surface and is described in the gear coordinate system O_g by $r(\xi_n, \zeta)$, and the surface normal by $\mathbf{n}(\xi_n, \zeta)$. The same point and surface normal is found in the tool coordinate system O_v by:

$$\mathbf{r}_v = \begin{pmatrix} \xi_v \\ \eta_v \\ \zeta_v \end{pmatrix} = \begin{pmatrix} \xi_\psi \cos \beta_c - \zeta_\psi \sin \beta_c \\ a - \eta_\psi \\ \xi_\psi \sin \beta_c + \zeta_\psi \cos \beta_c \end{pmatrix}; \text{ where } \begin{cases} \xi_\psi = \xi(\xi_n, 0) \cos \psi - \eta(\xi_n, 0) \sin \psi \\ \eta_\psi = \xi(\xi_n, 0) \sin \psi + \eta(\xi_n, 0) \cos \psi \\ \zeta_\psi = -Z \end{cases} \quad (6)$$

and

$$\mathbf{n}_v = \begin{pmatrix} n_{v,\xi} \\ n_{v,\eta} \\ n_{v,\zeta} \end{pmatrix} = \begin{pmatrix} n_{\psi,\xi} \cos \beta_c - n_{\psi,\zeta} \sin \beta_c \\ -\eta_{\psi,n} \\ n_{\psi,\xi} \sin \beta_c + n_{\psi,\zeta} \cos \beta_c \end{pmatrix}; \text{ where } \begin{cases} n_{\psi,\xi} = n_\xi(\xi_n, 0) \cos \psi - n_\eta(\xi_n, 0) \sin \psi \\ n_{\psi,\eta} = n_\xi(\xi_n, 0) \sin \psi + n_\eta(\xi_n, 0) \cos \psi \\ n_{\psi,\zeta} = n_\zeta \end{cases} \quad (7)$$

The gear tooth surface is here described in the transverse plane at $\zeta = 0$ in Equation 4. The gear profile at any other section, $\zeta \neq 0$, is found by pure rotation in O_g by the angle.

$$\Psi(\zeta) = \zeta \frac{\sin \beta}{z/2} \quad (8)$$

In Figure 4 the disc tool is shown with the contact point P described in the coordinate system O_v . The tool is a rotational symmetric surface, thus the resultant of the components $n_{v,\eta}$ and $n_{v,\zeta}$ of the normal vector \mathbf{n}_v must be directed through the rotational center. In conjunction with the point P's coordinates, for

which $\tan \gamma = \zeta_{v,p}/\eta_{v,p}$, the relation is obtained:

$$\tan \gamma = \frac{\zeta_{v,p}}{\eta_{v,p}} = \frac{n_{v,\zeta}}{n_{v,\eta}} \tag{9}$$

Rewriting to suit numerical calculations this relation will be:

$$E(\xi_n, \zeta) = \eta_{v,p}(\xi_n, \zeta) n_{v,\zeta}(\xi_n, \zeta) - \zeta_{v,p}(\xi_n, \zeta) n_{v,\eta}(\xi_n, \zeta) = 0 \tag{10}$$

For given ξ_n , the corresponding ζ value is obtained by solving Equation 10; here, Newton-Raphson's method is used.

$$\zeta_{i+1} = \zeta_i - \frac{E(\xi_n, \zeta)}{\frac{\partial E(\xi_n, \zeta)}{\partial \zeta}} \tag{11}$$

$$\frac{\partial E(\xi_n, \zeta)}{\partial \zeta} = \frac{\partial \eta_{v,p}(\xi_n, \zeta)}{\partial \zeta} n_{v,\zeta}(\xi_n, \zeta) + \eta_{v,p}(\xi_n, \zeta) \frac{\partial n_{v,\zeta}(\xi_n, \zeta)}{\partial \zeta} - \frac{\partial \zeta_{v,p}(\xi_n, \zeta)}{\partial \zeta} n_{v,\eta}(\xi_n, \zeta) - \zeta_{v,p}(\xi_n, \zeta) \frac{\partial n_{v,\eta}(\xi_n, \zeta)}{\partial \zeta} \tag{12}$$

A convergent solution gives the point of contact. By varying ξ_n ($\xi_1 \leq \xi_n \leq \xi_2$) all contacts between the gear and the tool are found. The line of contact is found by connecting these points. The tool axis is perpendicular to the gear axis for spur gears, hence the line of contact will be a coplanar curve and located in the transverse plane of the gear. However, for helical gears, the contact line will be a three-dimensional curve. The contact lines are shown in Figure 5 for a disc tool with the outer radius R_c , for a spur gear and a helical gear, $\beta = 20^\circ$.

With the contact line known, the cross-section of the form tool can be determined. The axial and radial coordinates of the disc cutter:

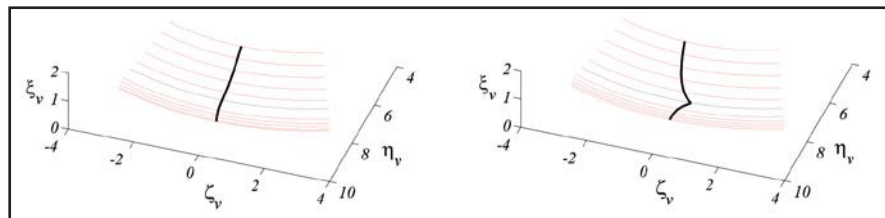


Figure 5 Contact lines.

$$\xi_c = \xi_v(\xi_n, \zeta) \tag{13}$$

$$\eta_c = \sqrt{\eta_v^2 + \zeta_v^2}$$

are revolved around the rotational axis a rotation angle ϕ to describe the disc tool

$$\xi_\phi = \xi_c \tag{14}$$

$$\eta_\phi = \eta_c \cos \phi$$

$$\zeta_\phi = \eta_c \sin \phi$$

A form milling wheel possesses a finite number of cutting teeth n . To avoid interference in the milling process, these cutting teeth must be relieved to allow only the cutting face to remove material. The cutting faces are described by planes intersecting the cutting teeth, perpendicular to the rotational axis, where the cutting edges are the boundaries of these faces. To describe a milling cutter, the complete wheel is gashed to the desired number of cutting teeth. The i :th cutting plane is then described by:

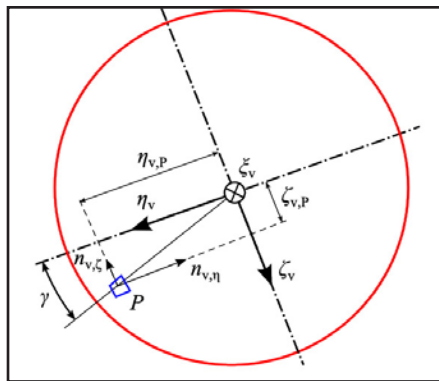


Figure 4 Form wheel.

$$\xi_{\phi,i} = \xi_c \tag{15}$$

$$\eta_{\phi,i} = \eta_c \cos(\phi + (i-1)\Delta\phi)$$

$$\zeta_{\phi,i} = \eta_c \sin(\phi + (i-1)\Delta\phi)$$

where $\Delta\phi = 2\pi/n$ is the equian-gular increment between the cutting faces.

For a form grinding wheel, there are no defined cutting edges. The surface grinding the gear tooth is the outer boundary of the form wheel. The form grinding process can then be described by a form milling

process with a sufficient number of cutting planes, so that the number of planes of the milling cutter does not influence the tooth surface topography. Then a milling cutter with many cutting faces is approximately equivalent to a grinding wheel.

Milling Process

The form wheel is now positioned to machine the gear. Like before, the tool is positioned at the center distance a and the rotational axis is set at the angle β_c to the transverse plane of the gear. It is not evident how the angle β_c should be chosen since the helical angle of a helical gear varies with the radius according to the relation $r_i \cot \beta_i = \text{constant}$. It is here assumed that the angle β_c coincides with the helical angle β of the gear at the pitch radius R_p . The form wheel can be positioned at another angle $\beta_c \neq \beta$, as long as the angle β_c corresponds to a radius on the gear tooth. However, the geometry of the form wheel must be determined at the same angle β_c as previously to machine the helical profile correctly.

The form wheel is rotated with the angular velocity ω_c to machine the gear here in the negative ϕ direction. Climb milling is achieved by moving the gear blank the distance $Z = -S_0\phi/(2\pi)$ at the angular displacement of ϕ , where $S = S_0m_n$ is the feed rate in distance-per-revolution. To achieve conventional milling, the feed is in the reversed direction, i.e. $-Z = S_0\phi/(2\pi)$.

Here the center of the cutting plane $i = 1$, ($\xi_{\phi,1} = 0, \eta_{\phi,1} = \eta_c$) is assumed to be located so it coincides with the center point of the gear ($\xi = \zeta = 0$ and $Z = 0$). In the mathematical model, the form wheel is now rotated backwards and the gear blank moves the distance Z and rotates $\psi(Z)$ so that the form wheel is outside the range of the gear blank. The form wheel then starts to machine the gear blank over the whole width. That means as no radial feed is present, the form wheel starts to machine the gear at full depth.

As the gear blank is fed the distance Z , the coordinates of the i :th cutting edge of the form wheel can be determined in the transverse plane of the gear. Simultaneously and continuously, the gear is rotated the angle $\psi(Z)$. The i :th cutting edge can then be represented in a coordinate system that coincides with that of the gear.

Table 1 Numerical example	
Gear	
Number of teeth	$z = 27$
Normal module	$m_n = 5 \text{ mm}$
Normal pressure angle	$\alpha_n = 20^\circ$
Tip radius	$R_{0,\text{tip}} = z/2/\cos\beta + x + 1$
Helical angle	$\beta = 25.8^\circ$
Addendum	$h_{0,a} = h_f/m_n = 1.25$
Addendum correction	$x = -0.1$
Rack fillet radius	$r_{0,r} = r_f/m_n = 0.2$
Form Cutter	
Number of cutting teeth	$n = 7$
Feed per revolution	$S_0 = S/m_n = 2.1/5 = 0.42$

Table 2 Radial run-out of tooth tips							
Cutting tooth number	1	2	3	4	5	6	7
Radial run-out [mm]	51.958	51.946	51.969	51.982	51.975	51.961	51.956
Deviation [μm]	-24	-36	-13	0	-7	-21	-26

(16)

$$r_{Si} = \begin{pmatrix} \xi_{Si}(\xi_{n,c}, \phi) \\ \eta_{Si}(\xi_{n,c}, \phi) \\ \zeta_{Si}(\xi_{n,c}, \phi) \end{pmatrix} = \begin{pmatrix} \zeta_\psi \cos \psi + \eta_\psi \sin \psi \\ -\xi_\psi \sin \psi + \eta_\psi \cos \psi \\ \zeta_\psi + Z \end{pmatrix}; \text{ where } \begin{cases} \xi_\psi = \xi_{\phi,i} \cos \beta_c + \zeta_{\phi,i} \sin \beta_c \\ \eta_\psi = a - \eta_{\phi,i} \\ \zeta_\psi = -\xi_{\phi,i} \sin \beta_c + \zeta_{\phi,i} \cos \beta_c \end{cases}$$

The Machined Surface

The machined tooth surface, that is, the surface after all material is removed, is now to be determined. By using a milling cutter with finite number of cutting teeth n that is fed by the feed rate S_0 , the machined surface will deviate from the ideal smooth geometry. The distance $h_0 = h/m_n$ between these two surfaces is measured in the normal direction from the ideal tooth surface to the machined surface. From a specific point on the gear tooth, the distance h_0 to the i :th cutting edge is found:

$$r_{Si}(\xi_{n,c}, \phi) = r(\xi_{n,c}, \zeta) - h_0 \frac{n(\xi_{n,c}, \zeta)}{|n|} \quad (17)$$

where $r(\xi_{n,c}, \zeta)$ is the coordinate of the ideal tooth surface and $n(\xi_{n,c}, \zeta)$ is the normal to this surface. The distance h_0 is measured in the normal direction from the ideal tooth surface and, in this formulation, measured positive in the direction into the gear blank material. In component form Equation 17 is expressed as:

$$f_\xi(\xi_{n,c}, \phi, h_0) = \xi_{Si}(\xi_{n,c}, \phi) + h_0 \frac{n_\xi(\xi_{n,c}, \zeta)}{|n|} - \xi(\xi_{n,c}, \zeta) = 0 \quad (18)$$

$$f_\eta(\xi_{n,c}, \phi, h_0) = \eta_{Si}(\xi_{n,c}, \phi) + h_0 \frac{n_\eta(\xi_{n,c}, \zeta)}{|n|} - \eta(\xi_{n,c}, \zeta) = 0$$

$$f_\zeta(\xi_{n,c}, \phi, h_0) = \zeta_{Si}(\xi_{n,c}, \phi) + h_0 \frac{n_\zeta(\xi_{n,c}, \zeta)}{|n|} - \zeta(\xi_{n,c}, \zeta) = 0$$

This set of equations contains three unknowns, namely, $\xi_{n,c}$, ϕ and h_0 . To find a solution, Newton-Raphson's method is employed. In matrix form, a solution is found by:

$$\begin{pmatrix} \xi_{n,c,k+1} \\ \phi_{k+1} \\ h_{0,k+1} \end{pmatrix} = \begin{pmatrix} \xi_{n,c,k} \\ \phi_k \\ h_{0,k} \end{pmatrix} - M^{-1} \begin{pmatrix} f_\xi(\xi_{n,c,k}, \phi_k, h_{0,k}) \\ f_\eta(\xi_{n,c,k}, \phi_k, h_{0,k}) \\ f_\zeta(\xi_{n,c,k}, \phi_k, h_{0,k}) \end{pmatrix} \quad (19)$$

where

$$M = \begin{pmatrix} \frac{\partial f_\xi}{\partial \xi_{n,c}} & \frac{\partial f_\xi}{\partial \phi} & \frac{\partial f_\xi}{\partial h_0} \\ \frac{\partial f_\eta}{\partial \xi_{n,c}} & \frac{\partial f_\eta}{\partial \phi} & \frac{\partial f_\eta}{\partial h_0} \\ \frac{\partial f_\zeta}{\partial \xi_{n,c}} & \frac{\partial f_\zeta}{\partial \phi} & \frac{\partial f_\zeta}{\partial h_0} \end{pmatrix} = \begin{pmatrix} \frac{\partial \xi_{Si}}{\partial \xi_{n,c}} & \frac{\partial \xi_{Si}}{\partial \phi} & \frac{\partial \xi_{Si}}{\partial h_0} \\ \frac{\partial \eta_{Si}}{\partial \xi_{n,c}} & \frac{\partial \eta_{Si}}{\partial \phi} & \frac{\partial \eta_{Si}}{\partial h_0} \\ \frac{\partial \zeta_{Si}}{\partial \xi_{n,c}} & \frac{\partial \zeta_{Si}}{\partial \phi} & \frac{\partial \zeta_{Si}}{\partial h_0} \end{pmatrix} \quad (20)$$

Reaching a convergent solution the distance from the ideal surface to the surface machined by the i :th cutting edge is known.

To find the finished machined surface, the surface after all material to be removed is cut, the maximum h_0 of all n cutting edges is to be found.

$$h_0(\xi_{n,c}, \zeta) = \max(h_0(\xi_{n,c}, \phi, i)) \quad (21)$$

In the machining process, all cutting teeth do not have the possibility to machine the surface at all positions. To make the calculations faster, only the cutting teeth facing the gear blank need to be considered.

Numerical Example and Validation

Table 1 shows the specifications of the gear and the milling cutter used in this example. The geometry of the milling cutter used in the simulation software is based on the mathematical model, whereas the indexable milling cutter used in experiments is determined using the software *PTM/GH-Precision Tool Manufacturing/Gear Hob*.

To verify the model, an actual gear is cut using an indexable insert milling cutter in a Höfler HF600. Before machining, the milling cutter was control measured for radial run-out at tooth tips. These values are given in Table 2, showing the maximum deviation of $36 \mu\text{m}$ between the cutting teeth. This run-out error is too large for the calculated results from the simulation model to agree with the observed machined surface topography. Thus, deviations must be considered in the model. To account for both axial and radial deviations, Δa_i and Δr_i , of the i :th cutting tooth, Equation 15 is modified accordingly:

$$\begin{aligned} \xi_{\phi,i} &= \xi_c + \Delta a_i \\ \eta_{\phi,i} &= (\eta_c + \Delta r_i) \cos(\phi + (i-1)\Delta\phi) \\ \zeta_{\phi,i} &= (\eta_c + \Delta r_i) \sin(\phi + (i-1)\Delta\phi) \end{aligned} \quad (22)$$

To compare the machined surface with the computed tooth surface from the simulation model, one tooth of the gear was cut

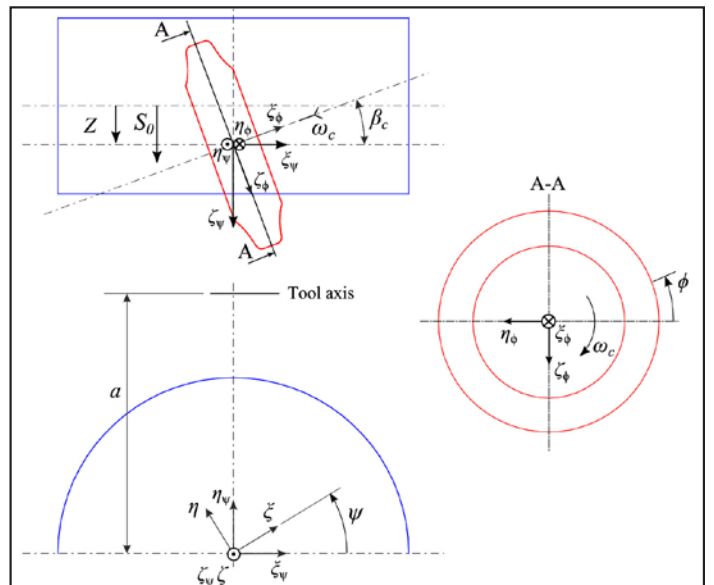


Figure 6 Form wheel machines helical gear.

out and a width of approximately 10 mm was scanned using a computer controlled optical microscope, Alicona Infinite Focus. The magnification used on the optical microscope was 20x, with a vertical resolution (height) of 25 nm and a lateral resolution (in-plane) of 3 μm.

The same area was calculated using the simulation model and the results are presented in Figure 7. In these figures, measurements along the three lines over the width are extracted, i.e. — lines a, b and c. The roughness profiles for these three lines are presented in Figure 8. The feed rate was set to $S=2.1\text{ mm/rev}$ in the axial direction of the gear, and the milling cutter having $n=7$ cutting teeth. Thus, the distance between the feed ridges of the feed marks should be approximately $s=S/n/\cos\beta=2.1\text{ mm}/7/\cos 25.8^\circ\approx 0.33\text{ mm}$. This is not the case in the results shown in Figure 8. Although all cutting teeth remove material in the milling process, the finished gear tooth is actually formed by only one cutting tooth due to the radial run-out error of the cutter, i.e. $s=S/\cos\beta=2.1\text{ mm}/\cos 25.8^\circ\approx 2.33\text{ mm}$.

Conclusion

This paper presents a mathematical model for determining the tooth surface topography machined by a form wheel, i.e. for both form grinding wheels and form milling cutters. The geometry of the form wheel is determined through inverse calculation

and the form wheel is able to manufacture helical gears correctly. Due to the finite number of cutting teeth of the milling cutter, the cut surface will deviate from the ideal smooth tooth surface. With this model the machine surface is predicted. To be able to predict the machined tooth surface topography is of great industrial interest as it opens up the manufacturing process for optimizations such as choosing process data and the required amount of grinding stock. In the prescribed mathematical model, the machined surface in both the fillet and involute region is determined.

The model is validated by milling a helical gear using an indexable insert milling cutter. This type of cutter could cause positional errors of the cutting teeth that are not present for conventional high speed steel milling cutters; such errors are axial and radial positional errors. The mathematical model is modified to account for these types of positional errors to the cutting teeth. Measurements of the positional errors of the used indexable milling cutter were used as input to the simulation model, resulting in very good agreement of the surface roughness achieved of the milled gear and the calculated roughness from the mathematical model.

Acknowledgement. This work is financially supported by SSF/ ProViking and SPI. The experimental work was performed at Sandvik Coromant in Sandviken, Sweden. The authors gratefully acknowledge the assistance. 

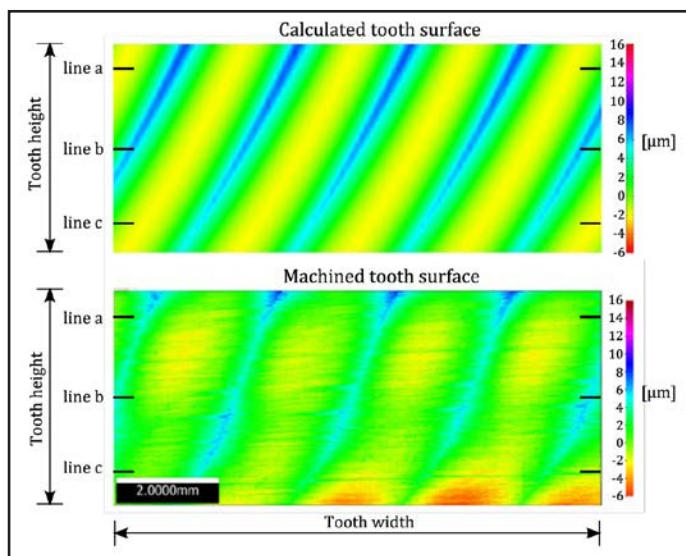


Figure 7 Comparison between the calculated and the machined tooth surface topography.

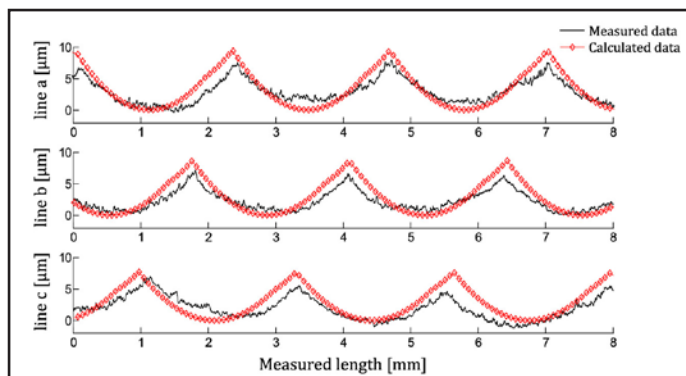


Figure 8 Comparison of line measurements between the calculated and the machined.

References

- Dudley, D.W. *Gear Handbook, The design, Manufacture, and Application of Gears*, 1962, Mc Graw-Hill.
- Ishibashi, A. and H. Yoshino. "Design and Manufacture of Gear Cutting Tools and Gears with an Arbitrary profile," *JSME International Journal*, 30, 1987, 1159-1166.
- Ehrmann, K.F. "Grinding wheel profile definition for the manufacture of drill flutes," *Annals of the CIRP*, 39, 1990, 153-156.
- Steth, D.S and S. Malkin. "CAD/CAM for Geometry and Process Analysis of Helical Groove Machining," *CIRP*, 39, 1990, 129-132.
- Xiao, D.C. and D. Lee. "A Contact Point Method for the Design of Form Cutters for Helical Gears," *ASME Journal of Engineering for Industry*, 1994, 116, 387-391.
- Häussler, U. "Generalistere Berechnung räumlicher Verzahnungen und ihre Anwendung auf Wälzfräserherstellung und Wälzfräsen," (In German), Ph. D. thesis, 1999, Universität Stuttgart.
- Shih, Y-P and S-D Chen. "Free-Form Flank Correction in Helical Gear Grinding Using a Five-Axis Computer Numerical Control Gear Profile Grinding Machine," *ASME Journal of Manufacturing Science and Engineering*, 2012, 134, 041006-1– 041006-13.
- Vedmar, L. "A Parametric Analysis of the Gear Surface Roughness after Hobbing," *ASME Journal of Mechanical Design*, 132, 2010, 111004-1–111004-8.
- DIN 867 (1986). Basic Rack Tooth Profiles for involute teeth of Cylindrical Gear for General Engineering and Heavy Engineering.

Carin Andersson is a Professor at the Division of Production and Materials in the Department of Mechanical Engineering, Lund University, Sweden.



Mattias Svahn is a Ph. D student at the Division of Machine Elements in the Department of Mechanical Engineering, Lund University, Sweden.



Lars Vedmar is an Associate Professor at the Division of Machine Elements in the Department of Mechanical Engineering, Lund University, Sweden.

